Proceedings of the 2018 13th World
Congress on Intelligent Control and Automation
July 4-8, 2018, Changsha, China

# A Novel Tele-operated Flexible Manipulator Based on the da-Vinci Research Kit

Chengzhi Song, Ivan Shuenshing Mok, Philip Waiyan Chiu and Zheng Li

***Abstract*—Flexible manipulators is now attracting an increasing interest in the field of minimally invasive surgery (MIS). Compared to rigid instruments, they could work in confined space and go through tortuous passes. The constrained tendon-driven serpentine mechanism (CTSM) is one of the novel flexible mechanisms proposed recently. It could provide a larger workspace and more dexterous distal end manipulation. In this paper, a number of flexible instruments were developed based on the CTSM and tele-operation was achieved by using the the da Vinci Research Kit (DVRK). The developed flexible instruments successfully completed the tasks that are commonly used in MIS training, including peg transfer and knotting.**

***Index Terms*—Flexible manipulator, da Vinci Research Kit, Minimally Invasive Surgery, Tele-operation**

## I. Introduction

Minimally Invasive Surgery(MIS)[1][2][3] is becoming the standard of care in most of surgical procedures due to the advantages of less blood loss, less pain, shorter hospital stay and better cosmesis. With the assistance of the robot, such as the da Vinci Surgical System, surgeons can now perform MIS much easier. This tele-operated system allows the surgeon to sit in front of the console and operating the patient side manipulator (PSM) using the master manipulator (MTM). One criticism of the robot is that the system is bulky. This is mainly attributed to its rigid instruments at the PSM. To access the targeted areas in the surgical site, the PSM and the rigid instruments need to pivot about the remote center of motion (RCM), which is often set around the incision port. As the length inserted into the surgical cavity is short and the length outside is much longer, the robot needs a large operation space[4][5].

On the other hand, flexible manipulators have the potential to address these limitations. The flexible manipulator could bend its backbone to reach the desired locations. This could expand the workspace inside the body cavity and reduce the operation space outside. Commonly used flexible manipulator design include the tendon/cable/wire-driven manipulator (TM)[6][7][8], the concentric tube manipulator (CTM)[9]and the hybrid design. The TM could be further divided into the tendon-driven serpentine manipulator (TSM), of which the backbone is made by a chain of short vertebrae, and the tendon-driven continuum manipulator (TCM), of which the backbone is a continuum beam. Among all the designs, the TSM shows the largest payload ability. This made it most promising in MIS[5]. Conventional TSM such as the one presented in [7] comprises of a chain of short vertebrae with two adjacent vertebrae forming a joint. Each of the joint could bend a small angle. However, by combining all the joint's rotation, the backbone deformation could be large. In the TSM, the length of the backbone is constant. Therefore, for a single-segment TSM, the distal end trajectory locates on a curved surface. To extend its workspace and enhance its distal end dexterity, a novel constrained tendon-driven flexible mechanism (CTSM) is proposed by Li et al[10]. In this mechanism, the flexible section is bent by the controlling cables, which is the same as in conventional TSMs. However, by using a concentric rigid constraint, the length of the bending section could be controlled. By adding one more degree of freedom (DOF), this design largely extends the distal end workspace and the distal end dexterity. More importantly, the size is not increased compared to the TSMs.

The da Vinci Research Kit (DVRK)[11] is an open source platform for research of MIS robots. The DVRK contains the PSMs and MTMs of the first generation of the da Vinci surgical system. It serves as an ideal platform for testing new

Fig. 1: The CTSM based Flexible Manipulator on the PSM

This work is supported by the Hong Kong General Research Fund (GRF/RGC) with project No. 14212316, Hong Kong Innovative Technology Fund (ITF) with project No. ITS/019/15, and CUHK-SJTU Joint Research Collaboration Fund

Chengzhi Song, is with the department of surgery, the Chinese University of Hong Kong. (Email: Songchengzhi@link.cuhk.edu.hk)

Ivan Shuenshing Mok is with the department of biomedical engineering, the Chinese University of Hong Kong. (Email:1155062836@link.cuhk.edu.hk )

Philip Waiyan Chiu is with the department of surgery and Chow Yuk Ho Technology Centre for Innovative Medicine, the Chinese University of Hong Kong. (Email: philipchiu@surgery.cuhk.edu.hk)

Zheng Li is with the department of surgery and Chow Yuk Ho Technology Centre for Innovative Medicine, the Chinese University of Hong Kong. (Email: lizheng@cuhk.edu.hk; Phone: +852-3505 1882)

978-1-5386-7346-1/18/$31.00 © 

instrument designs. In this work, we developed a number of flexible instruments based on the CTSM and achieved the tele-operation using the DVRK. To test the functionality of the developed instruments, we adopted the training tasks in the FLS (Fundamentals of Laparoscopic Surgery)[12]. In the FLS, five basic tasks are defined. These include the 'peg transfer', 'precision cutting', 'ligating loop', 'suture with extracorporeal knot' and 'suture with introcorporeal knot'. Among all the tasks, the peg transfer and knotting are most frequently used. Therefore, we select these two tasks to evaluate the developed instruments.

The rest of the paper is organized as follows: section II introduces the design of the CTSM based flexible instruments; section III presents the kinematic modeling; section IV focuses on the implementation and control in the tele-operation; section V gives the test results and section VI concludes the paper.

## II. Design and Prototyping

The design of the flexible manipulator contains two parts. The first part is the flexible section and the second part is the back-end interface.

### A. Design of the flexible section

The design of the flexible section is based on our previous TSM designs[7][13].

As shown in Fig.2, the backbone contains a number of identical vertebrae, with two adjacent vertebrae forming a joint. An elastic tube is in the central lumen of the backbone. It constrains the rotation of the joints and inhibits the twist. Therefore, each joint has two DOFs and the angle of each joint is assumed equal. The joint rotations are controlled by four cables, which pass through the pin holes evenly distributed on the vertebrae. An additional rigid tube is inserted into the elastic tube. It could translate along the backbone axis. Therefore, this rigid tube serves as another constraint and can control the length of bending section[10]. The working principle is shown in Fig.3.

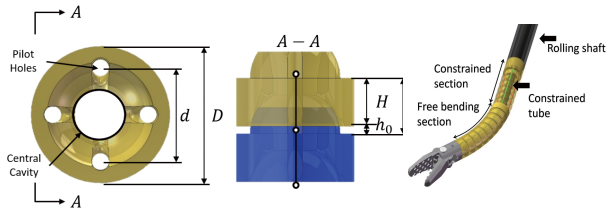


(a) Vertebrae (b) CTSM

Fig. 2: Design of the CTSM instrument

### B. Design of the back-end interface

In the DVRK, the instruments have four DOFs and these DOFs are controlled by four rotating discs respectively, as shown in Fig.4a. In the developed flexible instruments, there are five DOFs. These include: 1) end-effector motion; 2) shaft rolling; 3) flexible section pitch; 4) flexible section yaw and 5) constrain insertion. Therefore, the back-end interface needs be redesigned. In the design, the four rotating discs are used to control the first four DOFs and we used a stepper motor to control the fifth DOF, i.e. the translation of the rigid constraint. The design is illustrated in Fig.4b. To fully control the length of the bending section, the rigid tube translation range is the same as that of the flexible section. Therefore, the length of the back-end interface is extended. In the design, the weight of the back-end interface is minimized to reduce the side effect of the added weight of the instrument.

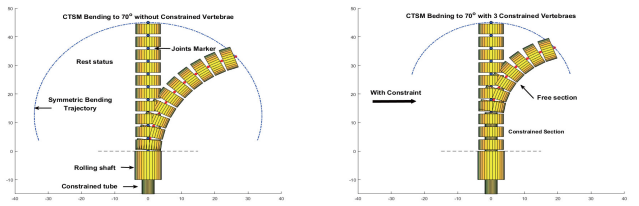


(a) Bending without constraint (b) Bending with reduced length

Fig. 3: CTSM bending illustration

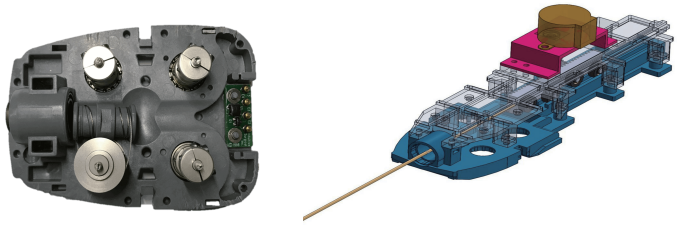

(a) original back-end of the da Vinci surgical instrument (b) CAD model of the back-end design for CTSM

Fig. 4: Design back-end for CTSM

### C. Prototyping of the flexible instrument

The designed instruments was 3D printed and assembled as shown in Fig.5. In the flexible instrument, there are a total of 10 vertebrae and 10 joints (first joint is formed with the shaft). The length of the flexible section is $L = 46mm$(varies with the constrained ), and the maximum bending angle is $150^o$. The total length of the flexible instrument is $668.6mm$ and the weight is $305.6g$ with motor components. For the original rigid instruments used in the DVRK(*Large Needle Driver Instrument*), the length is $500.0mm$ and the weight is $170.2g$.

## III. Kinematic Modeling

The Kinematic modeling of the CTSM is based on the piece-wise constant curvature (PCC) assumption. The nomenclature is shown in TABLE I and the coordinate frame setting is illustrated in Fig.6.

The kinematic modeling involves the mapping between the four spaces, i.e., 'motor space', 'cable space', 'joint space' and 'task space'. These mappings are illustrated in Fig.7. The kinematic model of the flexible bending section is described in [10][7]. In this paper, we focus on the kinematic integration of the flexible bending section and the PSM.

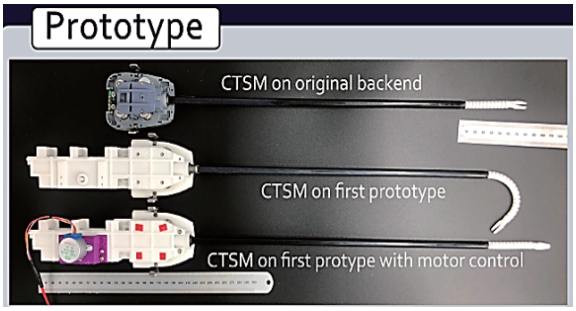


Fig. 5: Prototype of the CTSM instrument

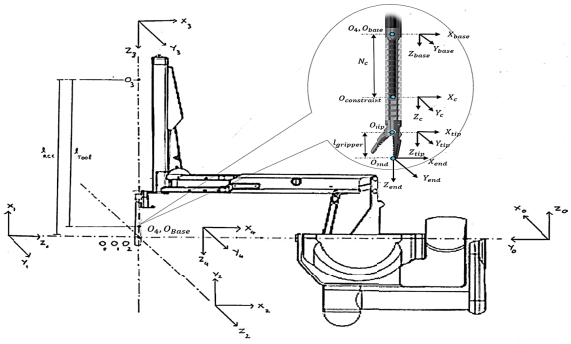

Fig. 6: Coordinate Frame System

TABLE I: Nomenclature

| | |
|---|---|
| $i$ | Index of flexible link/segment(within this paper i=1) |
| $j$ | Index of actuation wire/cable, $j$=l,r,u,d ... |
| $d$ | Distance between the actuation wire/cables = 6.5 mm |
| $\theta_{m,k}$ | Motor position of the $k$-th motor |
| $\vec{X}$ | Task space variables. $\vec{X}$ includes both the position vector $\vec{P}$ and pointing direction vector $\vec{\omega}$ with amplitude equals to angle |
| $\vec{\psi}$ | CTSM configuration space variables. $\vec{\psi}_i$ represents the variables for the $i$-th CTSM link. |
| $\vec{\theta}_m$ | Motor space variables |
| $\vec{P}_i$ | Tip position vector of $i$-th flexible link, where $\vec{P}_i = [P_{i,x}, P_{i,y}, P_{i,z}]^T$ |
| $R_i$ | Rotational matrix of the $i$-th flexible link in the $i$-th frame |
| $\vec{P}_e$ | End point position vector of the $i$-th flexible link in the base frame $\{0\}$ |
| $J_{X\psi}$ | Jacobian matrix maps the CTSM configuration space velocities to task space velocities, i.e. $\dot{\vec{X}}_i = J_{x\psi}\dot{\vec{\psi}}_i$ |
| $J_{\psi l}$ | Jacobian matrix maps the tendon/cable space velocities to Arc Geometry configuration space velocities, i.e. $\dot{\vec{\psi}}_i = J_{\psi l}\dot{\vec{l}}_i$ |
| $J_{l\theta_m}$ | Jacobian matrix maps the motor space velocities to the Cable space velocities, i.e. $\dot{\vec{l}}_i = J_{l\theta_m}\dot{\vec{\theta}}_m$ |
| $f_{x\psi}$ | Forward kinematics maps the CTSM configuration space variables to the task space variables, i.e. $\vec{x}_i = f_{x\psi}(\vec{\psi}_i)$ |
| $f_{\psi l}$ | Forward kinematics maps the Cable length vector to the CTSM configuration space variables, i.e. $\vec{\psi}_i = f_{\psi l}(\vec{l}_i)$ |
| $f_{l\theta_m}$ | Forward kinematics maps the motor space variables to the Cable space variables, i.e. $\vec{l}_i = f_{l\theta_m}(\vec{\theta}_m)$ |

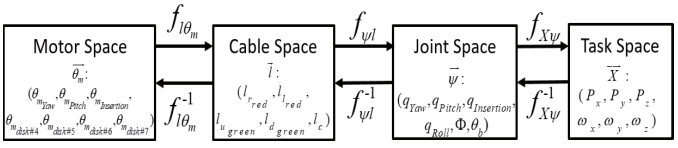


Fig. 7: The four kinematic mappings

The PSM is a serial link manipulator with three DOFs, i.e. the outer yaw, outer pitch and I/O insertion. The flexible instruments add five additional DOFs, i.e., the outer roll, gripping, the rigid constraint translation and the two directional bending of the flexible section. A hybrid D-H table is formed as in II. In this D-H table, we integrate the rigid constraint translation and the two directional bending of the flexible section as the joint 'CTSM'. The transformation matrix of the 'CTSM' joint is shown by transformation matrix ${}^{tip}T_{base}$.By generating the hybrid DH-table, transformation matrix from frame $F_0$ to frame $F_{tip}$ can be calculated as follows. For the PSM without the flexible instrument, the forward kinematic model is:

$$ {}^{base}T_0 = {}^{base}T_3 \cdot {}^3T_2 \cdot {}^2T_1 \cdot {}^1T_0 \tag{1} $$

For the PSM together with the flexible instrument, the forward kinematic model is:

$$ {}^{tip}T_0 = {}^{tip}T_{base} \cdot {}^{base}T_3 \cdot {}^3T_2 \cdot {}^2T_1 \cdot {}^1T_0 \tag{2} $$

TABLE II: Hybrid DH-table

| Frame | Joint name | Joint type | $a$ | $\alpha$ | $D$ | $\theta$ | $\Phi$ | $\theta_b$ | $N_c$ |
|---|---|---|---|---|---|---|---|---|---|
| 1 | Outer Yaw | 1 | 0 | $\frac{\pi}{2}$ | 0 | $q_1+\frac{\pi}{2}$ | 0 | 0 | 0 |
| 2 | Outer Pitch | 1 | 0 | $-\frac{\pi}{2}$ | 0 | $q_2+\frac{\pi}{2}$ | 0 | 0 | 0 |
| 3 | I/O Insertion | 2 | 0 | $\frac{\pi}{2}$ | $q_3-l_{rcc}$ | 0 | 0 | 0 | 0 |
| 4 | Outer Roll | 1 | 0 | 0 | $l_{tool}$ | $q_4$ | 0 | 0 | 0 |
| Base | CTSM | 3 | 0 | 0 | 0 | $\frac{\pi}{4}$ | $q_\Phi$ | $q_{\theta_b}$ | $q_{N_c}$ |
| Tip | Gripper | 0 | 0 | 0 | $l_{gripper}$ | 0 | 0 | 0 | 0 |

1 for revolute joint type
2 for prismatic joint type
3 for flexible joint type
0 for fixed joint type

The inverse kinematics of the PSM together with the flexible manipulator could be solved numerically as in [5]. In the solution, the Jacobian of the manipulator is critical. It is defined as $J_{X\psi}$ and it involves two parts, i.e., the PSM rigid joint Jacobian $J_{rig}$ and the flexible joint Jacobian $J_{flex}$. The full Jacobian is obtained as:

$$ J_{X\psi} = \begin{bmatrix} J_{rig} & J_{flex} \end{bmatrix} \tag{3} $$

where,

$$ J_{rig} = \begin{bmatrix} z_0 \times (P_{tip} - p_0) & z_1 \times (P_{tip} - p_1) & z_2 & z_3 \times (P_{tip} - p_3) \\ z_0 & z_1 & 0 & z_3 \end{bmatrix} \tag{4} $$

The Jacobian of the flexible instrument includes the linear component and the angular component.

$$ J_{flex} = \begin{Bmatrix} J_v \\ J_\omega \end{Bmatrix} \tag{5} $$

The linear component could be calculated by differentiating the position of the tip in the base frame as:

$$ J_v = \begin{bmatrix} \frac{\partial x_t}{\partial \Phi} & \frac{\partial x_t}{\partial \theta_b} & \frac{\partial x_t}{\partial N_c} \\ \frac{\partial y_t}{\partial \Phi} & \frac{\partial y_t}{\partial \theta_b} & \frac{\partial y_t}{\partial N_c} \\ \frac{\partial z_t}{\partial \Phi} & \frac{\partial z_t}{\partial \theta_b} & \frac{\partial z_t}{\partial N_c} \end{bmatrix} \tag{6} $$

For the angular component, it could be obtained by introducing the skew-symmetric matrix $S$ is introduced when computing $J_\omega$.

$$S(t) = \dot{R}(t)R^T(t) = \begin{bmatrix} 0 & -\omega_x & \omega_y \\ \omega_x & 0 & -\omega_z \\ -\omega_y & \omega_z & 0 \end{bmatrix}, \quad J_\omega = \begin{bmatrix} \omega_x \\ \omega_y \\ \omega_z \end{bmatrix} \tag{7}$$

Therefore, the components within matrix $J_\omega$ with respect to variable $\Phi$, $\theta_b$ and $N_c$ are represented as:

$$J_\omega(\Phi) = \begin{bmatrix} -cos\Phi sin\Theta_b \\ -sin\Phi sin\Theta_b \\ 1 - cos\Theta_b \end{bmatrix}, \quad J_\omega(\theta_b) = \begin{bmatrix} -N_f \cdot sin\Phi \\ N_f \cdot cos\Phi \\ 0 \end{bmatrix}, \quad J_\omega(N_c) = \begin{bmatrix} 0 \\ 0 \\ 0 \end{bmatrix} \tag{8}$$

The following algorithm shows how to solve the differential inverse kinematics with the developed kinematic models [14].

**Algorithm 1:** Differential Inverse Kinematics Solution

**Input :** Desired Cartesian values in Transformation matrix form $X_{dsr}$, initial guess $q_0$, and model structure $m$

**Output:** $q_{next}$

```
func (q_next) = Inverse Kinematics (X_dsr, q_0, m);
cycle_limit = 5000;
X_err = 1;
while (cycle < cycle_limit) do
    q_next = q_0;
    if abs(X_err) > 0 then
        q_next = q_next + δq;
        X_act = Forward Kinematics(q_next, m);
        X_err = X_dsr − X_act;
    else
        return q_next;
    end
end
```

## IV. Control of the Flexible Manipulator

The developed flexible instrument is installed onto the PSM of the DVRK and controlled by the MTMs, using tele-operation. Figure 8 shows the overall framework for the tele-operation.

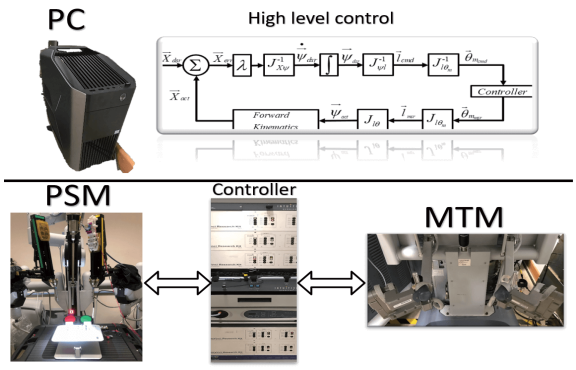


Fig. 8: Illustration of Framework for Tele-operation

In the tele-operation framework, the desired trajectory of the end-effector is obtained from the MTM. The PC solves the differential inverse kinematics and the controller commands the motor's motion of the slave arm.The control loop for the slave arm is as shown in Fig.9.

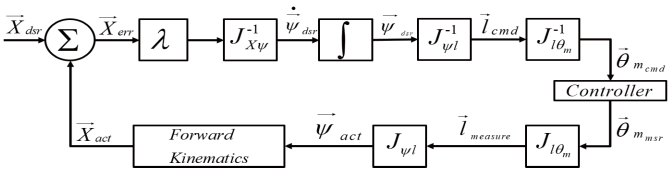


Fig. 9: Framework of the Control loop for slave end

It is noted that, in the DVRK, the operation of the MTM is fully aligned with the PSM by an offset matrix $R_{offset}$. This matrix is given as:

$$R_{offset} = \begin{bmatrix} -1 & 0 & 0 \\ 0 & -1 & 0 \\ 0 & 0 & 1 \end{bmatrix} \tag{9}$$

## V. Results

### A. Verification of Kinematics model in MATLAB®

Forward kinematics maps the CTSM configuration space variables to the task space variables - $\vec{x}_i = f_{x\psi}(\vec{\psi}_i)$ and its inverse mapping are verified in MATLAB, simulation results are shown in Fig.10:

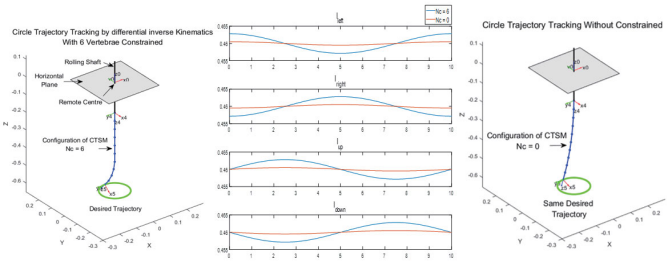


Fig. 10: Cable change Comparison for CTSM with different Bending Section

### B. Experimental evaluation

To test the developed flexible instruments, we set up the DVRK as shown in Fig.11. In the figure, the left part shows the PSM, the middle is the controller and the right part is the master console. Two flexible instruments were installed onto the PSMs of the DVRK. The endoscope was held by the endoscopic camera manipulator (ECM) of the DVRK. The endoscope view was transmitted to the eye pieces in the console. One could sit in front of the console and operate the MTM by looking into the eye pieces. The insertion of the constraint is controlled by a custom made foot pedal placed under the MTM. In the MIS training, there are five tasks defined by the FLS. These tasks include the peg transfer, precision cutting, ligating loop, intracoporeal knotting and extracoporeal knotting. Among all the tasks, the ligating loop and extracoporeal knotting need to involve other instruments, while the precision cutting involves the scissors or cautery

hook. Therefore, in the evaluation, we choose the two tasks that could be completed by the developed flexible instruments alone.

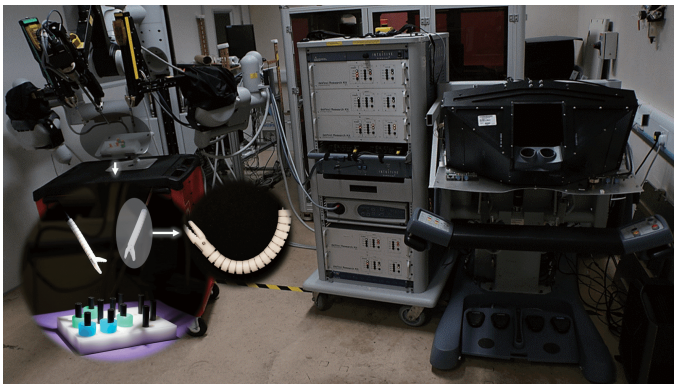

Fig. 11: Tele-operation experiments Setup

The test results are shown in Fig.12. In the figure, the image sequence shows the instruments movement during the tasks. The tests show that the developed flexible instruments could successfully complete the tasks under the visual guidance from the endoscope.

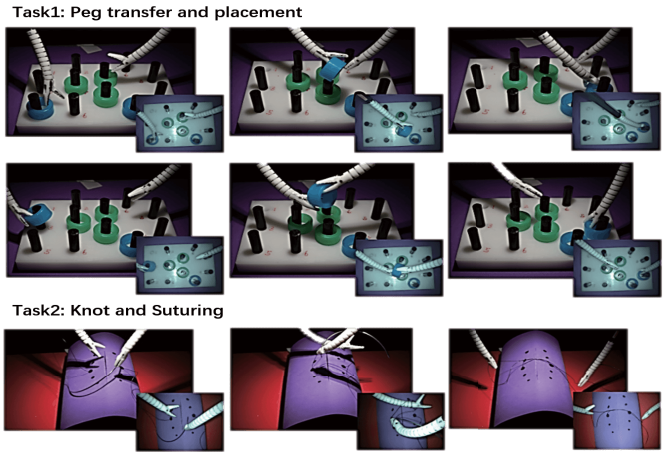


Fig. 12: Tele-operation experiments

## VI. Conclusion

In this work, we presented the design, modeling and prototyping of the flexible instruments based on the CTSM. The instruments are integrated into the DVRK. Tele-operation of the flexible instruments is achieved. By using the developed flexible instruments, we completed the common tasks used in the MIS training. These include the peg transfer and the knotting. From this work, we see the potential of flexible instruments in general MIS. However, issues such as payload enhancement, shape sensing, etc. remains to be solved before the flexible instruments could benefit the patients.

## References


[1] J. Burgner-Kahrs, D. C. Rucker, and H. Choset, "Continuum robots for medical applications: A survey," *IEEE Transactions on Robotics*, vol. 31, no. 6, pp. 1261–1280, 2015.

[2] R. H. Sturges Jr and S. Laowattana, "A flexible, tendon-controlled device for endoscopy," *The International journal of robotics research*, vol. 12, no. 2, pp. 121–131, 1993.

[3] H. Ren, C. M. Lim, J. Wang, W. Liu, S. Song, Z. Li, G. Herbert, Z. T. H. Tse, and Z. Tan, "Computer-assisted transoral surgery with flexible robotics and navigation technologies: A review of recent progress and research challenges," *Critical Reviews in Biomedical Engineering*, vol. 41, no. 4-5, 2013.

[4] Z. Li, H. Yu, H. Ren, P. W. Chiu, and R. Du, "A novel constrained tendon-driven serpentine manipulator," in *Intelligent Robots and Systems (IROS), 2015 IEEE/RSJ International Conference on*. IEEE, 2015, pp. 5966–5971.

[5] Z. Li, L. Wu, H. Ren, and H. Yu, "Kinematic comparison of surgical tendon-driven manipulators and concentric tube manipulators," *Mechanism and machine theory*, vol. 107, pp. 148–165, 2017.

[6] R. J. Webster III and B. A. Jones, "Design and kinematic modeling of constant curvature continuum robots: A review," *The International Journal of Robotics Research*, vol. 29, no. 13, pp. 1661–1683, 2010.

[7] Z. Li and R. Du, "Design and analysis of a bio-inspired wire-driven multi-section flexible robot," *International Journal of Advanced Robotic Systems*, vol. 10, no. 4, p. 209, 2013.

[8] J. Burgner, D. C. Rucker, H. B. Gilbert, P. J. Swaney, P. T. Russell, K. D. Weaver, and R. J. Webster, "A telerobotic system for transnasal surgery," *IEEE/ASME Transactions on Mechatronics*, vol. 19, no. 3, pp. 996–1006, 2014.

[9] P. E. Dupont, J. Lock, B. Itkowitz, and E. Butler, "Design and control of concentric-tube robots," *IEEE Transactions on Robotics*, vol. 26, no. 2, pp. 209–225, 2010.

[10] Z. Li, H. Ren, P. W. Y. Chiu, R. Du, and H. Yu, "A novel constrained wire-driven flexible mechanism and its kinematic analysis," *Mechanism and Machine Theory*, vol. 95, pp. 59–75, 2016.

[11] P. Kazanzides, Z. Chen, A. Deguet, G. S. Fischer, R. H. Taylor, and S. P. DiMaio, "An open-source research kit for the da vinci® surgical system," in *2014 IEEE International Conference on Robotics and Automation (ICRA)*. IEEE, 2014, pp. 6434–6439.

[12] C. A. Ragle and B. A. Fransson, "Fundamental laparoscopic skills," *Advances in equine laparoscopy. Ames, Iowa: Wiley-Blackwell*, pp. 13–20, 2012.

[13] Z. Li, R. Du, M. C. Lei, and S. M. Yuan, "Design and analysis of a biomimetic wire-driven robot arm," in *ASME 2011 International Mechanical Engineering Congress and Exposition*. American Society of Mechanical Engineers, 2011, pp. 191–198.

[14] M. Yip and N. Das, "Robot autonomy for surgery," *arXiv preprint arXiv:1707.03080*, 2017.